

Drosophila Salt-inducible Kinase (SIK) Regulates Starvation Resistance through cAMP-response Element-binding Protein (CREB)-regulated Transcription Coactivator (CRTC)*[§]

Received for publication, March 2, 2010, and in revised form, November 30, 2010. Published, JBC Papers in Press, December 2, 2010, DOI 10.1074/jbc.C110.119222

Sekyu Choi^{‡§}, Wonho Kim^{‡§}, and Jongkyeong Chung^{§¶||1}

From the [‡]Department of Biological Sciences, Korea Advanced Institute of Science and Technology, 335 Gwahangno, Yuseong-Gu, Daejeon 305-701 and the [§]National Creative Research Initiatives Center for Energy Homeostasis Regulation, [¶]Institute of Molecular Biology and Genetics, and ^{||}School of Biological Sciences, Seoul National University, San 56-1, Sillim-Dong, Gwanak-Gu, Seoul 151-742, Republic of Korea

Salt-inducible kinase (SIK), one of the AMP-activated kinase (AMPK)-related kinases, has been suggested to play important functions in glucose homeostasis by inhibiting the cAMP-response element-binding protein (CREB)-regulated transcription coactivator (CRTC). To examine the role of SIK *in vivo*, we generated *Drosophila* SIK mutant and found that the mutant flies have higher amounts of lipid and glycogen stores and are resistant to starvation. Interestingly, SIK transcripts are highly enriched in the brain, and we found that neuron-specific expression of exogenous SIK fully rescued lipid and glycogen storage phenotypes as well as starvation resistance of the mutant. Using genetic and biochemical analyses, we demonstrated that CRTC Ser-157 phosphorylation by SIK is critical for inhibiting CRTC activity *in vivo*. Furthermore, double mutants of SIK and CRTC became sensitive to starvation, and the Ser-157 phosphomimetic mutation of CRTC reduced lipid and glycogen levels in the SIK mutant, suggesting that CRTC mediates the effects of SIK signaling. Collectively, our results strongly support the importance of the SIK-CRTC signaling axis that functions in the brain to maintain energy homeostasis in *Drosophila*.

Salt-inducible kinase (SIK)² was first cloned from adrenal glands of rats fed with a high salt diet (1), and its transcription was strongly induced by membrane depolarization in the brain (2). Recent studies unexpectedly demonstrated that SIK1 also plays important functions in liver glucose homeostasis (3) and survival of myocytes (4). Furthermore, SIK1 is involved in TGF- β signaling (5) and histone deacetylase regulation (6), supporting highly diverse functions in mammalian systems.

* This work was supported by National Creative Research Initiatives Grant 2010-0018291 from the Korean Ministry of Education, Science and Technology.

[§] The on-line version of this article (available at <http://www.jbc.org>) contains supplemental Figs. 1–8, Tables 1–2, and Experimental Procedures.

¹ To whom correspondence should be addressed: School of Biological Sciences, Seoul National University, San 56-1, Sillim-Dong, Gwanak-Gu, Seoul 151-742, Republic of Korea. Tel.: 82-2-880-4399; Fax: 82-2-876-4401; E-mail: jkc@snu.ac.kr.

² The abbreviations used are: SIK, salt-inducible kinase; CRE, cAMP-response element; CREB, cAMP-response element-binding protein; CRTC, CREB-regulated transcription coactivator; AMPK, AMP-activated protein kinase; Dilp, *Drosophila* insulin-like peptide; AKH, adipokinetic hormone.

Through genomic database analyses, SIK2 (Qin-induced kinase (QIK)) and SIK3 (QSK) were identified as SIK family members based on their structural homologies to SIK1 (7). Interestingly, SIK family kinases belong to AMP-activated protein kinase (AMPK)-related kinases, which are activated by LKB1 (8, 9). Based on this conserved regulation of SIK and other AMPK-related kinases, SIK is believed to have highly specialized downstream targets to differentially function in the cell. However, due to the lack of loss-of-function animal models, the *in vivo* functions of SIK remain elusive, in contrast to the well characterized functions of AMPK.

The members of CREB-regulated transcription coactivator (CRTC), also known as TORC (transducer of regulated CREB), are newly identified CREB co-activators (10, 11). Under the basal condition, phosphorylated CRTC is sequestered in the cytoplasm. However, in response to increased levels of calcium and cAMP, CRTC is dephosphorylated and subsequently translocated to the nucleus, which leads to the activation of cAMP-response element (CRE)-mediated gene transcription by association with CREB (12, 13). Recent studies demonstrated that one of the family members, CRTC2, has a crucial function in the gluconeogenic program in the liver (3, 14). SIK and AMPK repress CRE transcriptional responses by phosphorylating CRTC2 at Ser-171 and keep the transcription factor in the cytoplasm (3, 13). In the case of *Drosophila*, increases in insulin signaling inhibit CRTC through phosphorylation under the fed condition (15). Also, activated *Drosophila* CRTC can stimulate CREB target genes (15), supporting evolutionarily highly conserved functions of CRTC in metazoans.

In this study, we describe the generation and characterization of SIK-deficient flies and demonstrate that SIK activity in the brain is required for the regulation of lipid and glycogen level in the body. We also show that SIK mutation increases starvation resistance. Finally, we demonstrate that CRTC and CREB dominantly mediate these *in vivo* functions of SIK.

EXPERIMENTAL PROCEDURES

Fly Stocks—The following fly stocks were obtained from the Bloomington Stock Center: *hs-Gal4*, *gmr-Gal4*, *elav-Gal4*, and *cg-Gal4*. CRTC²⁵⁻³ was kindly provided by Dr. M. Montminy (15). UAS-CREB^{RNAi} (line 101512) and UAS-AMPK α ^{RNAi} (line 1827) were obtained from the Vienna Dro-

sophila RNAi Center. *SIK*^{Δ41} was generated by the imprecise excision of the *SIK*^{G366} line (Korea Advanced Institute of Science and Technology (KAIST) *Drosophila* Library Facility, Daejeon, Korea). All flies were grown on standard cornmeal-yeast-agar medium at 25 °C.

Generation of Transgenic Fly Strains—To generate *UAS-SIK* flies, *SIK* EST cDNA (Berkeley *Drosophila* Genome Project accession number RH42017) was cloned into the Myc-tagged pUAST vector and microinjected into *W*¹¹¹⁸ embryos. Full-length CRTC cDNA was generated by reverse transcription-PCR (RT-PCR). The PCR-cloned CRTC was then subcloned into the NotI-XhoI site of the FLAG-tagged pUAST vector.

Site-directed Mutagenesis—For site-directed mutagenesis, the QuikChangeTM kit (Stratagene) was used. For generation of a kinase-dead mutant SIK (K170M, SIK^{KM}), 5'-GAAC-GAGGTGGCTATCATGATCATTGACAAGTGC-3' and 5'-GCGACTTGTCAATGATCATGATAGCCACCTCG-TTC-3' primers were used. For generation of a CRTC mutant non-phosphorylatable by SIK (S157A, CRTC^{S157A}), 5'-GCG-GCGGTCCAGCGCCGATTCGGCGC-3' and 5'-GCGC-CGAATCGGCGCTGGACCGCCGC-3' primers were used. For generation of a CRTC mutant mimicking SIK-dependent phosphorylation (S157D, CRTC^{S157D}), 5'-GTGGCGGCGGT-CCAGCGACGATTCGGCGC-3' and 5'-GCGCCGAATCG-TCGCTGGACCGCCGCCAC-3' primers were used.

Quantitative Real-time PCR—Dissected tissues of larvae and adults were collected, and RNA was extracted using an RNeasy mini kit (Qiagen). Total RNA (1 mg) was reverse-transcribed by M-MLV reverse transcriptase (Promega), and the generated cDNA was used for real-time RT-PCR (Bio-Rad iQ5 real-time PCR detection system) using 2 ng of cDNA template and a 500 nM primer concentration. The following primers were used to amplify the *SIK* transcript: 5'-CTCGC-GTCTTGTCCGACCCAATG-3' and 5'-GTATGCCAGCCA-AGGAGAGATCTTCG-3' (kinase domain); 5'-TCGGAGAA-GAAAGTTCT-3' and 5'-GCCACTGGACGAGCTACTACT-3' (C-terminal domain). Values were normalized to *rp49*. Results are expressed as arbitrary units, with the each value of salivary gland and abdomen considered as 1 unit.

Staining with Nile Red—The abdominal regions of female flies up to 5 days old were manually opened, and floating fat body cells were released into mounting medium (50% glycerol/PBS, 0.1% Triton X-100, Nile Red 1:55,000 (Sigma N3013)). Cells were analyzed within 4 h following mounting using a Zeiss LSM 510.

Immunoblot Analysis—Fly heads were lysed in lysis buffer (20 mM Tris-HCl (pH 7.5), 1% Triton X-100, 1 mM EDTA, 5 mM EGTA, 150 mM NaCl, 20 mM NaF, 1 μg/ml leupeptin, and 1 mM PMSF) for 30–60 min on ice. After centrifugation at 13,000 rpm for 15 min, the supernatant was reserved for protein determination and SDS-PAGE analysis. The antibodies used were anti-phospho-CRTC1 (Cell Signaling Technology, 3359), anti-FLAG-M2 (Cell Signaling Technology, 2368), anti-Myc (Cell Signaling Technology, 2272), and anti-β-tubulin (Developmental Studies Hybridoma Bank, E7).

Starvation Assay—For each genotype, 3–5-day-old female flies were transferred to vials of 1% agar/PBS with filter papers

soaked with distilled water, and dead flies were scored every 4 h.

Lipid and Glycogen Measurement—Total lipid and glycogen of adult females were measured using previously described methods (15–18).

Capillary Feeder Assay—We used previously reported experimental procedures with minor modifications (19).

Quantification Analysis—Student's *t* tests were used for comparisons between two groups. *p* < 0.05 was considered statistically significant. The *p* values given in the survival data are the result of a log rank test using GraphPad Prism 5 software.

RESULTS

Drosophila SIK shares considerable sequence homology with mammalian SIK1 and SIK2 in its kinase domain (supplemental Fig. 1). To assess the *in vivo* role of SIK, *SIK* loss-of-function mutants were generated by mobilizing the P element from *SIK*^{G366}. We found one allele, *SIK*^{Δ41}, with a 1,148-bp (X1953962–1955112) deletion in the *SIK* encoding region including the translation start site and the ATP-binding site of the kinase domain (Fig. 1, A and B). By precisely excising the P element, we obtained a revertant allele, *SIK*^{RV}, and used it as a genetically matched control for phenotypic analyses. *SIK* mRNA was not detected in *SIK*^{Δ41} (Fig. 1C and supplemental Fig. 2), confirming that it is a null mutant.

To examine the role of SIK in energy homeostasis, we characterized *SIK*^{Δ41} under feeding and fasting conditions. We found that 1-week-old *SIK*^{Δ41} mutant flies had higher amounts of lipid and stored glycogen when compared with those in *SIK*^{RV} controls, but the difference became more apparent after 24 h of starvation (Fig. 1, E and F). Furthermore, Nile Red staining of dissected fat body tissues displayed larger lipid droplets in *SIK*^{Δ41} mutants than those of *SIK*^{RV} controls (Fig. 1G). In contrast to increased lipid and glycogen storage, *SIK*^{Δ41} flies showed unnoticeable difference in body weight (Fig. 1D) and similar food intake when compared with *SIK*^{RV} controls according to the capillary feeder method (supplemental Fig. 3).

Previous studies in *Drosophila* have shown that starvation resistance correlates considerably with lipid contents (20). Therefore, we wondered whether the higher lipid and glycogen contents of *SIK*^{Δ41} mutant flies provide a better chance of survival during starvation. Under starvation conditions, the median and maximum survival times increased by 26 and 20%, respectively, in *SIK*^{Δ41} flies when compared with *SIK*^{RV} controls (Fig. 1H), supporting the idea that loss of *SIK* dramatically increased starvation resistance.

To identify the tissue distribution of SIK, we assessed the level of *SIK* transcripts in the third instar larvae. Interestingly, *SIK* expression levels were much higher in the brain than any other tissues (Fig. 2A). We also measured the expression pattern of *SIK* in adult body segments and also between adult male and female. Consistent with larval gene expression, *SIK* was highly expressed in the head and did not show sex-specific expression patterns (Fig. 2B). Collectively, these data suggest a role of *Drosophila* SIK in the nervous system.

SIK Regulates Starvation Resistance through CRTC

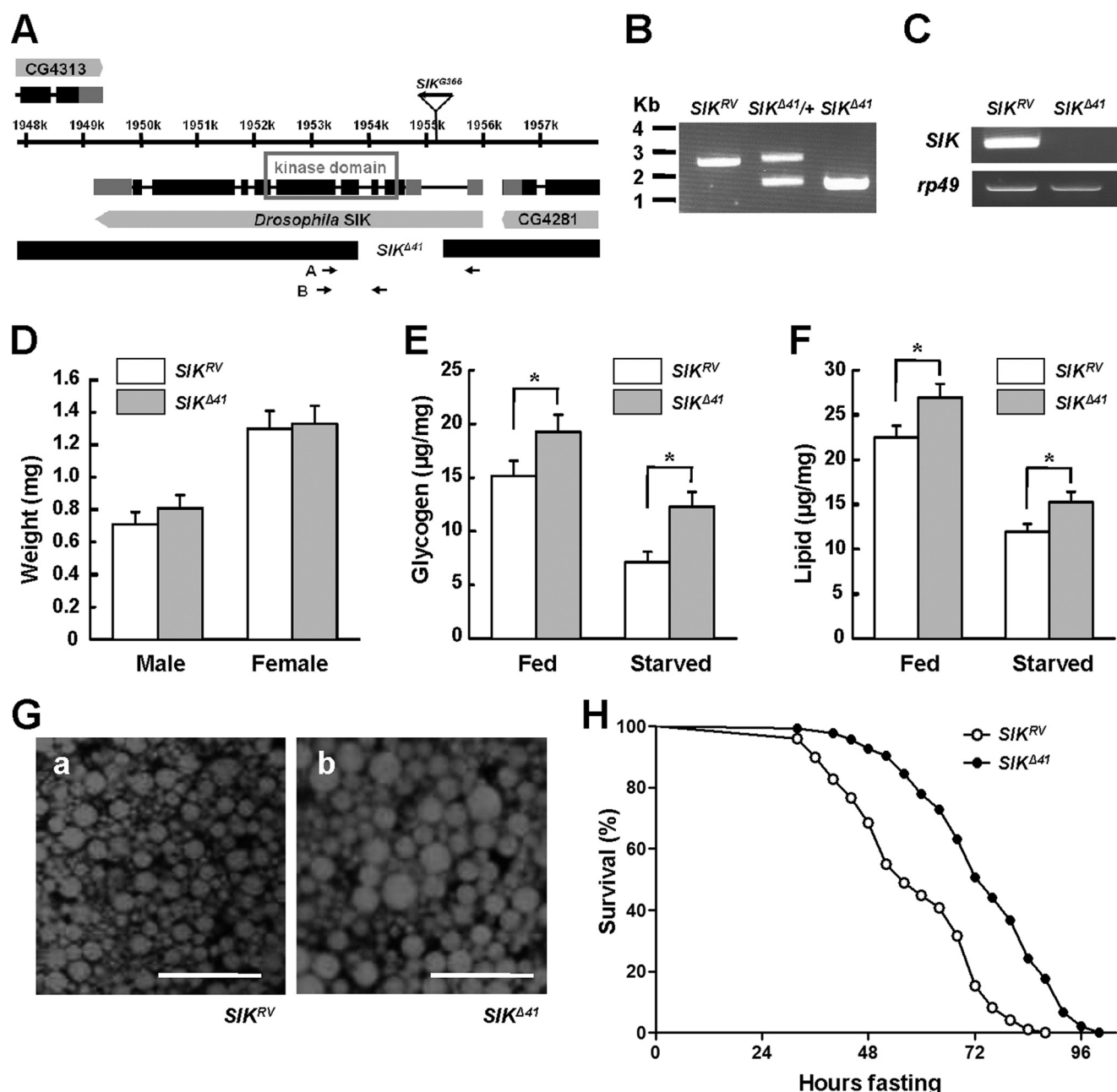


FIGURE 1. SIK mutants are resistant to starvation. *A*, genomic region of *SIK* locus. Exons of *SIK* are indicated by boxes, and coding regions are colored black. The deleted regions for *SIK*-null mutants (*SIK*^{Δ41}) are also presented. The gene expression of CG4313 and CG4281 is not affected in *SIK*^{Δ41} deletion (data not shown). *B*, PCR revealed deletion of genomic DNA in *SIK* revertants (*SIK*^{RV}), heterozygous *SIK* mutants (*SIK*^{Δ41/+}), and *SIK*^{Δ41} using the A primer set in *A*. *C*, RT-PCR analysis of *SIK* mRNA in *SIK*^{RV} and *SIK*^{Δ41} using the B primer set in *A*. *rp49* was used as a loading control. *D*, average weight of *SIK*^{RV} and *SIK*^{Δ41} adult flies (mean ± S.D., *n* = 60). *E*, total glycogen contents, expressed as μg/mg of body weight, in fed or 24-h starved *SIK*^{RV} and *SIK*^{Δ41} flies (mean ± S.D., *n* = 10; *, *p* < 0.05, Student's *t* test). *F*, total lipid contents in fed and 24-h starved *SIK*^{RV} and *SIK*^{Δ41} flies (mean ± S.D., *n* = 10; *, *p* < 0.05, Student's *t* test). *G*, Nile Red staining of fat bodies from *SIK*^{RV} (panel *a*) and *SIK*^{Δ41} (panel *b*) flies. Scale bar, 50 μm. *H*, relative survival rate in response to starvation of *SIK*^{RV} and *SIK*^{Δ41} female flies. The percentage of survival at different times is shown. *n* = 60; *p* < 0.05 (log rank test). Experiments were performed in triplicate.

To further study the gene expression patterns of *SIK*, we examined which body part of *SIK* expression can mediate metabolic regulation. We used *elav-Gal4* and *cg-Gal4* to drive pan-neuronal and fat body-specific expression of UAS-*SIK*, respectively. As shown in supplemental Fig. 4, *A* and *B*, exogenous *SIK* protein was successfully expressed in a tissue-specific manner.

Intriguingly, neuronal overexpression of *SIK* in a *SIK*^{Δ41} background reduced glycogen and lipid contents to a level

similar to those of *SIK*^{RV} control fly in both fed and starved conditions (Fig. 2, *C* and *D*, respectively). However, fat body expression of *Drosophila SIK* did not alter either of the metabolic contents (Fig. 2, *C* and *D*), suggesting that there could be specific roles of *SIK* in neurons.

To determine whether *SIK* expression is required in the nervous system or in the fat body regarding mediation of starvation resistance in *SIK* mutants, we performed genetic rescue experiments. A dramatic decrease in starvation re-

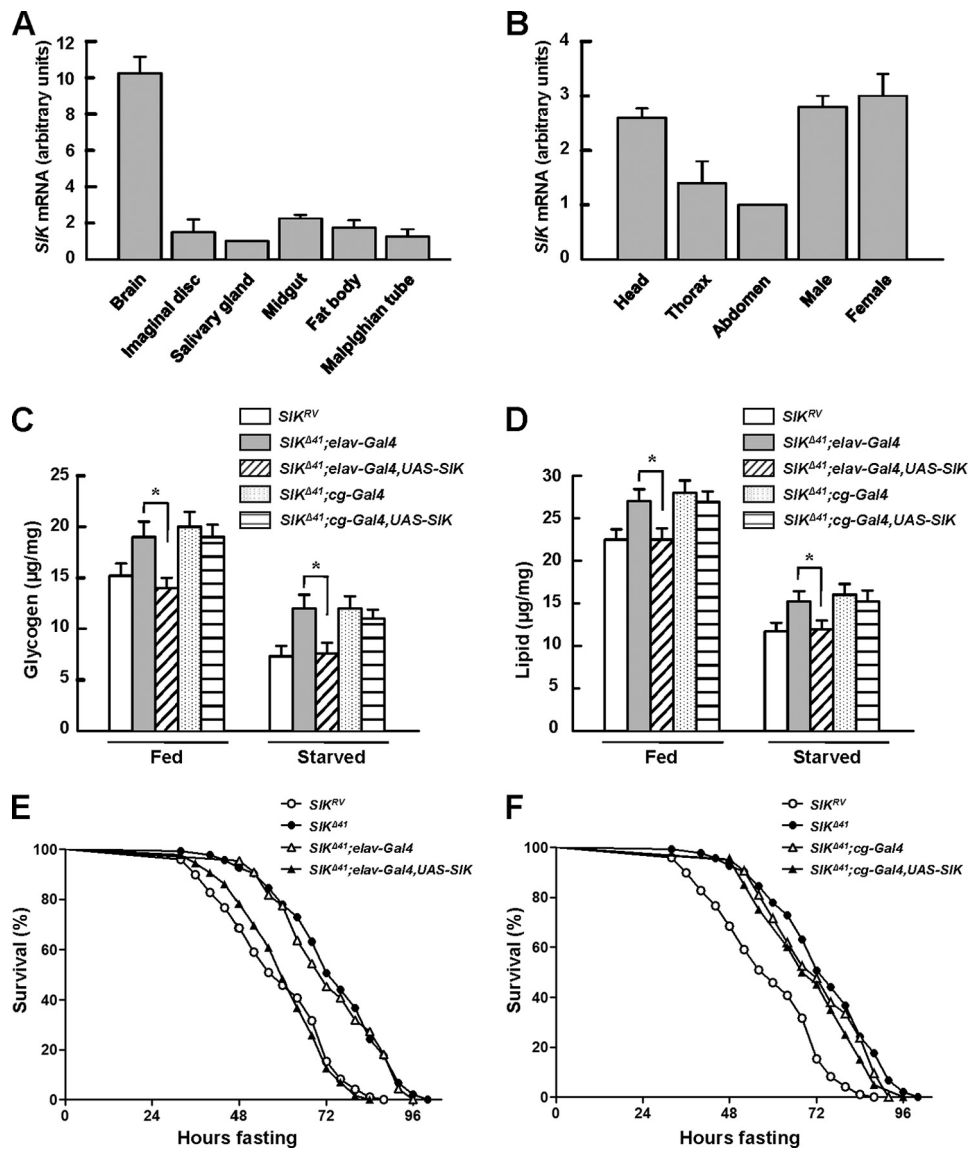


FIGURE 2. Neuronal SIK expression rescues starvation responses. A and B, the expression level of SIK was measured by quantitative real-time PCR analysis in larval (A) and adult tissues (B). Results are representative of three independent experiments and are expressed as arbitrary units (mean ± S.D.). C, total glycogen contents in fed and 24-h starved *SIK^{RV}* and *SIK^{Δ41}* flies, with and without driving expression of SIK constructs using *elav-Gal4* or *cg-Gal4* (mean ± S.D., *n* = 10; *, *p* < 0.05, Student's *t* test). D, total lipid contents in fed and 24-h starved *SIK^{RV}* and *SIK^{Δ41}* flies, with and without driving expression of SIK constructs using *elav-Gal4* or *cg-Gal4* (mean ± S.D., *n* = 10; *, *p* < 0.05, Student's *t* test). E, relative survival rate in response to starvation of *SIK^{RV}*, *SIK^{Δ41}*, *SIK^{Δ41};elav-Gal4* control, and *SIK^{Δ41};elav-Gal4,UAS-SIK* female flies. *n* = 60; *p* < 0.05 (log rank test). F, relative survival rate in response to starvation of *SIK^{RV}*, *SIK^{Δ41}*, *SIK^{Δ41};cg-Gal4* control, and *SIK^{Δ41};cg-Gal4,UAS-SIK* female flies. *n* = 60.

sistance to the level of *SIK^{RV}* controls was observed in *SIK*-null mutants after expressing exogenous SIK under the control of *elav-Gal4*, a neuronal driver, but not under the control of *cg-Gal4*, a fat body driver (Fig. 2, E and F, respectively).

Because mammalian SIK regulates target gene expression by directly phosphorylating CRTC and consequently inhibiting CRTC nuclear translocation (3, 13), we performed ommatidial assays to examine functional interactions and genetic epistasis between *Drosophila* SIK and CRTC. Previous studies have successfully used ommatidial assays to discover the relationship between CRTC and CREB in *Drosophila* (15). Although expression of the SIK wild type or kinase-dead form under the control of *gmr-Gal4*, an eye-specific driver, in wild type genetic background did not show any apparent pheno-

types (Fig. 3A, panels b and c, respectively), overexpression of CRTC using the *gmr-Gal4* driver in wild type background resulted in a rough eye phenotype with ommatidial loss (Fig. 3A, panel d). Interestingly, co-overexpression of SIK with CRTC caused partial rescue of the CRTC phenotype, restoring ommatidial structure and eye size (Fig. 3A, panel e), whereas the kinase-dead form of SIK did not (Fig. 3A, panel f), indicating that the kinase activity-dependent interaction between SIK and CRTC is conserved in *Drosophila*.

To confirm these genetic epistasis experiments further, we expressed the constitutive active CRTC S157A mutation, the counterpart of mammalian CRTC2 S171A (Fig. 3B), in the developing eye. Overexpression of CRTC S157A caused a more severe eye phenotype with loss of ommatidia and mechanosensory bristles (Fig. 3A, panel g) than the phenotypes

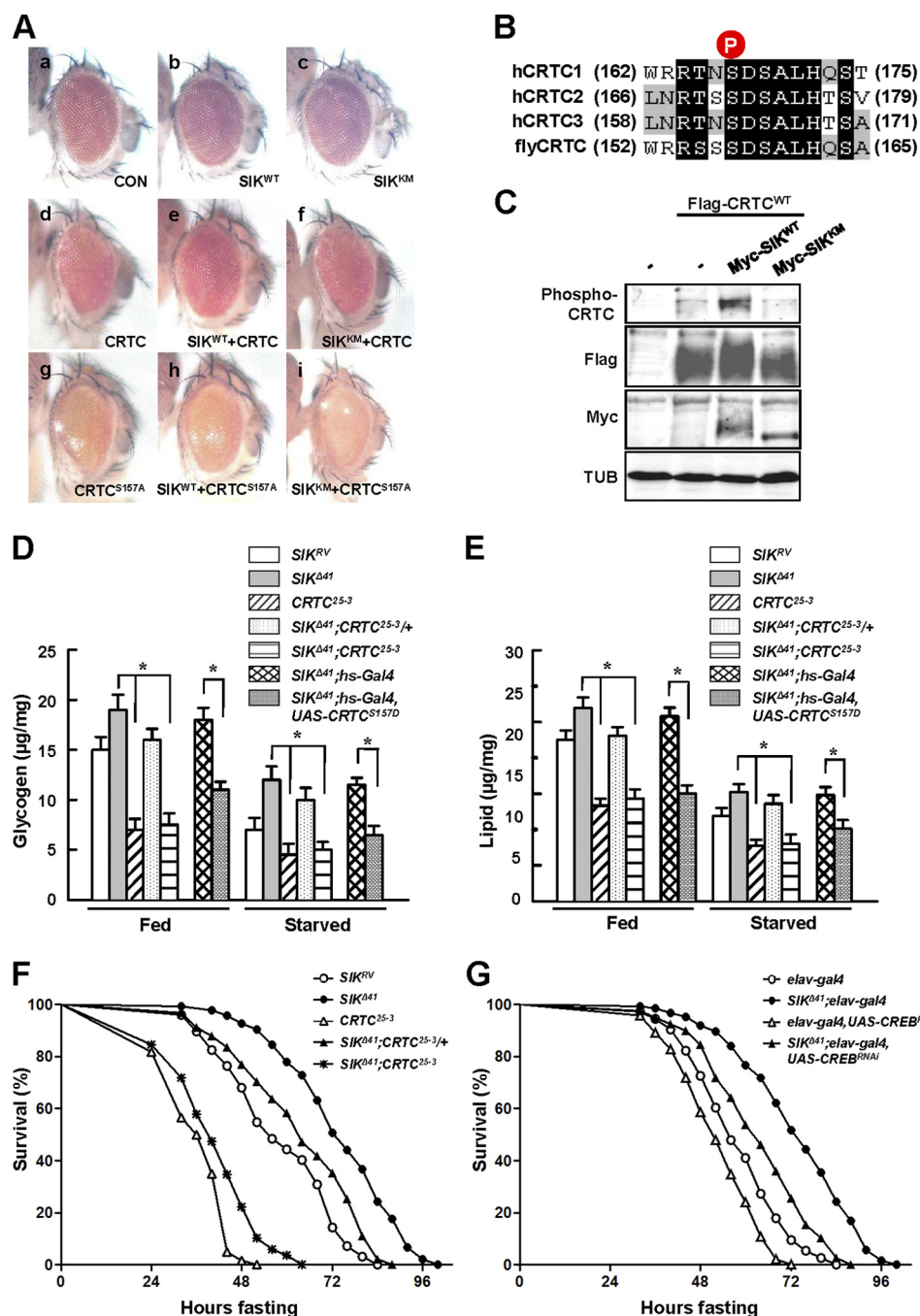


FIGURE 3. CRTC and CREB mediate the starvation responses of SIK. A, panels a–i, effects of indicated genotype expression in *Drosophila* eye. Genotypes are: *gmr-Gal4/+* (panel a), *gmr-Gal4/UAS-SIK^{WT}* (panel b), *gmr-Gal4/UAS-SIK^{KM}* (panel c), *gmr-Gal4/UAS-CRTC^{WT}* (panel d), *gmr-Gal4,UAS-CRTC^{WT}/UAS-SIK^{WT}* (panel e), *gmr-Gal4,UAS-CRTC^{WT}/UAS-SIK^{KM}* (panel f), *gmr-Gal4,UAS-CRTC^{S157A}/UAS-SIK^{WT}* (panel g), *gmr-Gal4,UAS-CRTC^{S157A}/UAS-SIK^{KM}* (panel i). CON, control. B, amino acid alignment of human CRTC1–3 and *Drosophila* CRTC at the SIK phosphorylation site (circled P). C, immunoblot analysis showing the effect of wild type and kinase-dead SIK on Ser-157 phosphorylation of CRTC protein in adult flies. TUB, tubulin. D, total glycogen contents in fed and 24-h starved SIK^{RV} , $SIK^{\Delta 41}$, $CRTC^{25-3}$, $SIK^{\Delta 41};CRTC^{25-3}/+$, $SIK^{\Delta 41};CRTC^{25-3}/+$, $SIK^{\Delta 41};hs-Gal4$, and $SIK^{\Delta 41};hs-Gal4,UAS-CRTC^{S157D}$ flies (mean \pm S.D., $n = 10$; $*$, $p < 0.05$, Student's *t* test). E, total lipid contents in fed and 24-h starved SIK^{RV} , $SIK^{\Delta 41}$, $CRTC^{25-3}$, $SIK^{\Delta 41};CRTC^{25-3}/+$, $SIK^{\Delta 41};CRTC^{25-3}$, $SIK^{\Delta 41};hs-Gal4$, and $SIK^{\Delta 41};hs-Gal4,UAS-CRTC^{S157D}$ flies (mean \pm S.D., $n = 10$; $*$, $p < 0.05$, Student's *t* test). F, relative survival rates in response to starvation of SIK^{RV} , $SIK^{\Delta 41}$, $CRTC^{25-3}$, $SIK^{\Delta 41};CRTC^{25-3}/+$, and $SIK^{\Delta 41};CRTC^{25-3}$ female flies. $n = 60$; $p < 0.05$ (log rank test). G, relative survival rate in response to starvation of *elav-Gal4*, $SIK^{\Delta 41};elav-Gal4$, *elav-Gal4,UAS-CREB^{RNAi}*, and $SIK^{\Delta 41};elav-Gal4,UAS-CREB^{RNAi}$ female flies. $n = 30$; $p < 0.05$ (log rank test).

found in wild type CRTC expression (Fig. 3A, panel d). Expectedly, co-overexpression of CRTC S157A with SIK failed to display any rescue of the defective ommatidia or mechanosensory bristles (Fig. 3A, panel h), indicating that this CRTC mutant does not respond to SIK signaling. To further confirm the interaction between SIK and CRTC, we

examined the phosphorylation status of CRTC using fly head extracts from the same lines used in Fig. 3A, panels d–f. Expression of SIK increased Ser-157 phosphorylation of CRTC in a kinase activity-dependent manner (Fig. 3C), demonstrating that SIK induces CRTC phosphorylation at the conserved Ser-157.

We also generated *SIK* and *CRTC* double mutants (*SIK*^{Δ41}; *CRTC*²⁵⁻³) to genetically confirm their functional interactions. Although removal of one copy of the *CRTC* gene decreased lipid and glycogen levels in fed and starved *SIK*^{Δ41} mutant, removal of both copies of *CRTC* in the *SIK* mutant background showed further decreased lipid and glycogen contents similar to *CRTC*-null mutant (Fig. 3, *D* and *E*).

To test whether Ser-157 residue of *CRTC* is critical in regulating lipid and glycogen content by *SIK*, we expressed *CRTC* S157D, which mimics the phosphorylated *CRTC* by *SIK*. Remarkably, *CRTC* S157D reduced lipid and glycogen levels in fed and starved *SIK*^{Δ41} mutant flies (Fig. 3, *D* and *E*).

Consistent with these lipid and glycogen phenotypes, as *CRTC* level decreased in the *SIK* mutant background, the flies became sensitive to starvation (Fig. 3*F*). Taken together, these data indicate that *CRTC* mediates the metabolic and starvation responses of *SIK* signaling.

CREB has been characterized to mediate *SIK*-*CRTC* signaling in mammals (21), and CREB activity is decreased in *Drosophila* *CRTC* mutant (15). We conducted genetic interaction experiments between *SIK* and CREB by knocking down neuronal CREB expression in the *SIK*-null background. As CREB level decreased in a *SIK* mutant background, the increased lipid stores and starvation resistance of the *SIK* mutant were strongly inhibited (Fig. 3*G* and supplemental Fig. 5, *B* and *C*). These results provide strong evidence to support that CREB is the critical target of *SIK*-*CRTC* signaling in *Drosophila*.

Finally, to figure out which hormonal or humoral factors regulate fat and glycogen contents, and supposedly *Drosophila* energy homeostasis in *SIK* signaling (supplemental Fig. 8), we conducted genome-wide microarray analyses on head mRNAs from fed and starved *SIK*^{Δ41} mutant flies relative to those of *SIK*^{RV} controls. This study revealed that 181 transcripts (fed condition) and 144 transcripts (starved condition) were significantly up-regulated in the mutant (≥2.0-fold) (supplemental Tables 1 and 2). Some of the affected genes are involved in stress responses and lipid metabolism. Many of the genes contain full CRE (TGACGTCA) and/or half-CRE (TGACG/CGTCA) consensus-binding site(s) within 3 kb upstream of the translational start site (supplemental Tables 1 and 2). These results again strongly support that *CRTC*-CREB-dependent gene expression is important to mediate *SIK* signaling in *Drosophila*.

DISCUSSION

SIK, one of the AMPK-related kinases, is involved in controlling fasting metabolism (3, 22). There is a single *Drosophila* orthologue for mammalian *SIK1* and *SIK2* (supplemental Fig. 1). Using the *Drosophila* model system, we discovered that neuronal *SIK* regulates metabolic indices, such as body contents of glycogen and lipid, by inhibiting *CRTC* transcriptional coactivator.

Mammalian *SIK* represses transcriptional responses mediated by CREB through phosphorylation and cytoplasmic retention of *CRTCs* (3, 13). Our results consistently demonstrated that *CRTC* Ser-157 residue, the counterpart of mammalian *CRTC2* Ser-171 residue, is structurally and functionally conserved for *SIK*-dependent phosphorylation (Fig.

3*B*). Because *SIK* expression did not influence *CRTC* S157A-induced phenotypes and *SIK* mutants became more sensitive to starvation by reducing gene dosages of *CRTC* (Fig. 3), we concluded that *CRTC* mediates starvation responses of *SIK* signaling in *Drosophila*. These studies also support that the functional interaction between *SIK* and *CRTC* is highly conserved throughout the evolution.

In starved condition, *SIK* and *CRTC* double mutants showed a higher starvation resistance than *CRTC* mutants (Fig. 3*F*). Based on our microarray data and previously published data, the regulated genes of *SIK* and *CRTC* are not completely overlapped (supplemental Table 2) (15). The results suggest that the unknown function of *SIK* can mediate the difference between *SIK*/*CRTC* double mutants and *CRTC* mutants.

CRTC-CREB functional interaction is also highly conserved in *Drosophila* (15). As decreased neuronal CREB level strongly suppressed increased lipid stores and starvation resistance of *SIK*-null mutant (Fig. 3*F* and supplemental Fig. 5, *B* and *C*), we suggest CREB as a main target for *SIK* signaling in *Drosophila*. Consistently, recent studies have shown that neuronal CREB activity regulates energy stores and starvation responses (23). Combining these results, neuronal CREB should be the key target of *SIK*-*CRTC* signaling in *Drosophila* (supplemental Fig. 8).

Because AMPK has been suggested as an upstream kinase of *CRTC* from mammalian studies (3, 24), we conducted experiments to examine whether neuronal AMPK is also related to the phenotypes of the *SIK* mutant. Interestingly, our experiments showed that neuron-specific knockdown of AMPK induced no significant effect on lipid and glycogen storage (supplemental Fig. 6, *B* and *C*). In addition, AMPK RNAi flies were not resistant to starvation (supplemental Fig. 6*D*), which is consistent with previous reports by others (25, 26). These results suggest that *SIK* but not AMPK is the dominant upstream regulator of *CRTC*-CREB signaling in *Drosophila* brain.

Metabolic storage is modulated by a variety of tissue-specific processes (27). Surprisingly, we found that the main gene expression pattern of *SIK* appears in the brain rather than in other metabolic tissues including the fat body, the functional equivalent of the mammalian liver and adipose tissue in *Drosophila* (Fig. 2*A*). Furthermore, *SIK* expression in neuronal tissue almost fully rescued increased storage of lipid and glycogen phenotypes of *SIK*-null mutants (Fig. 2, *C* and *D*). These results strongly support that neuronal *SIK* controls glycogen and lipid storage in some remote tissues such as the fat body (supplemental Fig. 8).

Based on our current data, it is important to figure out the communication method between brain and fat/glycogen under *SIK* regulation (supplemental Fig. 8). *Drosophila* brain has neurosecretory cells that secrete *Drosophila* insulin-like peptides (Dilps) and adipokinetic hormone (AKH, the insect glucagon) into the hemolymph (the insect blood) (28, 29). Recent studies showed that flies with mutations in the insulin signaling pathway have a moderate increase in lipid stores and are resistant to starvation (18, 29). In addition, AKH receptor mutant flies are impaired in fat storage and become resistant to

SIK Regulates Starvation Resistance through CRTC

starvation (30). Therefore, we have conducted quantitative PCR experiments to measure Dilps and AKH levels from *SIK* mutant head. Interestingly, we could not detect significant changes in Dilps and AKH expression (supplemental Fig. 7 and data not shown). Therefore, we suggest that neuronal *SIK* expression can change metabolic indices by regulating other hormones or humoral factors in *Drosophila* (supplemental Fig. 8).

In summary, we have demonstrated here that *SIK* is important in energy metabolism and starvation responses *in vivo*. Thereby *SIK* may be a potential therapeutic target for treating obesity and other metabolic diseases.

Acknowledgments—We thank Ayoung Kwak and Taeyoon Kyung for critical reading of the manuscript. We are grateful to M. Montminy for kindly providing reagents. We also thank the Bloomington Stock Center and *Drosophila* Genomics Research Center for kindly providing materials.

REFERENCES

1. Wang, Z., Takemori, H., Halder, S. K., Nonaka, Y., and Okamoto, M. (1999) *FEBS Lett.* **453**, 135–139
2. Feldman, J. D., Vician, L., Crispino, M., Hoe, W., Baudry, M., and Herschman, H. R. (2000) *J. Neurochem.* **74**, 2227–2238
3. Koo, S. H., Flechner, L., Qi, L., Zhang, X., Sreaton, R. A., Jeffries, S., Hedrick, S., Xu, W., Boussouar, F., Brindle, P., Takemori, H., and Montminy, M. (2005) *Nature* **437**, 1109–1111
4. Berdeaux, R., Goebel, N., Banaszynski, L., Takemori, H., Wandless, T., Shelton, G. D., and Montminy, M. (2007) *Nat. Med.* **13**, 597–603
5. Kowanetz, M., Lönn, P., Vanlandewijck, M., Kowanetz, K., Heldin, C. H., and Moustakas, A. (2008) *J. Cell Biol.* **182**, 655–662
6. van der Linden, A. M., Nolan, K. M., and Sengupta, P. (2007) *EMBO J.* **26**, 358–370
7. Okamoto, M., Takemori, H., and Katoh, Y. (2004) *Trends Endocrinol. Metab.* **15**, 21–26
8. Hardie, D. G., and Carling, D. (1997) *Eur. J. Biochem.* **246**, 259–273
9. Lizcano, J. M., Göransson, O., Toth, R., Deak, M., Morrice, N. A., Boudeau, J., Hawley, S. A., Udd, L., Mäkelä, T. P., Hardie, D. G., and Alessi, D. R. (2004) *EMBO J.* **23**, 833–843
10. Conkright, M. D., Canettieri, G., Sreaton, R., Guzman, E., Miraglia, L., Hogenesch, J. B., and Montminy, M. (2003) *Mol. Cell* **12**, 413–423
11. Iourgenko, V., Zhang, W., Mickanin, C., Daly, I., Jiang, C., Hexham, J. M., Orth, A. P., Miraglia, L., Meltzer, J., Garza, D., Chirn, G. W., McWhinnie, E., Cohen, D., Skelton, J., Terry, R., Yu, Y., Bodian, D., Buxton, F. P., Zhu, J., Song, C., and Labow, M. A. (2003) *Proc. Natl. Acad. Sci. U.S.A.* **100**, 12147–12152
12. Bittinger, M. A., McWhinnie, E., Meltzer, J., Iourgenko, V., Latario, B., Liu, X., Chen, C. H., Song, C., Garza, D., and Labow, M. (2004) *Curr. Biol.* **14**, 2156–2161
13. Sreaton, R. A., Conkright, M. D., Katoh, Y., Best, J. L., Canettieri, G., Jeffries, S., Guzman, E., Niessen, S., Yates, J. R., 3rd, Takemori, H., Okamoto, M., and Montminy, M. (2004) *Cell* **119**, 61–74
14. Dentin, R., Hedrick, S., Xie, J., Yates, J., 3rd, and Montminy, M. (2008) *Science* **319**, 1402–1405
15. Wang, B., Goode, J., Best, J., Meltzer, J., Schilman, P. E., Chen, J., Garza, D., Thomas, J. B., and Montminy, M. (2008) *Cell Metab.* **7**, 434–444
16. Van Handel, E. (1985) *J. Am. Mosq. Control Assoc.* **1**, 302–304
17. Van Handel, E. (1985) *J. Am. Mosq. Control Assoc.* **1**, 299–301
18. Broughton, S. J., Piper, M. D., Ikeya, T., Bass, T. M., Jacobson, J., Drieger, Y., Martinez, P., Hafen, E., Withers, D. J., Leever, S. J., and Partridge, L. (2005) *Proc. Natl. Acad. Sci. U.S.A.* **102**, 3105–3110
19. Ja, W. W., Carvalho, G. B., Mak, E. M., de la Rosa, N. N., Fang, A. Y., Liong, J. C., Brummel, T., and Benzer, S. (2007) *Proc. Natl. Acad. Sci. U.S.A.* **104**, 8253–8256
20. Djawdan, M., Chippindale, A. K., Rose, M. R., and Bradley, T. J. (1998) *Physiol. Zool.* **71**, 584–594
21. Katoh, Y., Takemori, H., Lin, X. Z., Tamura, M., Muraoka, M., Satoh, T., Tsuchiya, Y., Min, L., Doi, J., Miyauchi, A., Witters, L. A., Nakamura, H., and Okamoto, M. (2006) *FEBS J.* **273**, 2730–2748
22. Alessi, D. R., Sakamoto, K., and Bayascas, J. R. (2006) *Annu. Rev. Biochem.* **75**, 137–163
23. Iijima, K., Zhao, L., Shenton, C., and Iijima-Ando, K. (2009) *PLoS One* **4**, e8498
24. Dentin, R., Liu, Y., Koo, S. H., Hedrick, S., Vargas, T., Heredia, J., Yates, J., 3rd, and Montminy, M. (2007) *Nature* **449**, 366–369
25. Tohyama, D., and Yamaguchi, A. (2010) *Biochem. Biophys. Res. Commun.* **394**, 112–118
26. Johnson, E. C., Kazgan, N., Bretz, C. A., Forsberg, L. J., Hector, C. E., Worthen, R. J., Onyenwoke, R., and Brenman, J. E. (2010) *PLoS One* **5**, e137
27. Leopold, P., and Perrimon, N. (2007) *Nature* **450**, 186–188
28. Lee, G., and Park, J. H. (2004) *Genetics* **167**, 311–323
29. Rulifson, E. J., Kim, S. K., and Nusse, R. (2002) *Science* **296**, 1118–1120
30. Grönke, S., Müller, G., Hirsch, J., Fellert, S., Andreou, A., Haase, T., Jäckle, H., and Kühnlein, R. P. (2007) *PLoS Biol.* **5**, e137